JOM, Vol. 67, No. 1, 2015
DOI: 10.1007/s11837-014-1244-0

Hierarchical Bridging Between *Ab Initio* and Atomistic Level Computations: Calibrating the Modified Embedded Atom Method (MEAM) Potential (Part A)

M.F. HORSTEMEYER,[1,2,4,5] J.M. HUGHES,[1] N. SUKHIJA,[1] W.B. LAWRIMORE II,[1] S. KIM,[1] R. CARINO,[1] and M.I. BASKES[1,3]

1.—Center for Advanced Vehicular Systems, Mississippi State University, Starkville, MS 39759, USA. 2.—Department of Mechanical Engineering, Mississippi State University, Starkville, MS 39759, USA. 3.—Department of Aerospace Engineering, Mississippi State University, Starkville, MS 39759, USA. 4.—Predictive Design Technologies, Starkville, MS 39759, USA. 5.—e-mail: mfhorst@predictivedesigntech.com

This article provides a sequential calibration methodology for correlating the Modified Embedded Atom Method (MEAM) potential parameters to lower length scale calculation results or experimental data. We developed a graphical interactive MATLAB program called the MEAM Potential Calibration (MPC) tool that provides an interface with the large-scale atomistic/molecular massively parallel simulator. The MPC tool supports a rigorous yet fairly simple calibration methodology for determining the MEAM potential parameters. A pure aluminum system is used as an example to demonstrate the bridging methodology; however, the tool can be used for any material.

INTRODUCTION

Integrated Computational Materials Engineering (ICME), although a fairly recent label,[1] had its roots, philosophy, and practice occurring much earlier when *ab initio* and atomistic simulations were first studied in the 1980s. The ICME example that we focus on here arises from the engineering downscaling requirements related to plasticity (see Ref. 2 for a tutorial on downscaling and upscaling for the length scale bridging). Since the downscaling requirement from the macroscale is plasticity, the key simulations at the microscale are then dislocation dynamics, which require the dislocation mobilities from lower length scales (atomistic simulations). The downscaling requirements for the atomistic simulations are the atomic interfacial energies and elastic moduli from lower length scale simulations (*ab initio* simulations). After the downscaling requirements are established, the upscaling simulations and analyses can then be conducted. Here, we will not focus on the macroscale plasticity nor the microscale dislocation dynamics. One can review that work in Ref. [3] The focus here is with the atomic level model that garners information from *ab initio* Density Functional Theory (DFT) simulations but still focuses on the dislocation pertinent parameters in model calibration.

A widely used atomic level model is the Modified Embedded Atom Method (MEAM) proposed by Baskes.[4,5] The MEAM potential was based on the Embedded Atom Method (EAM)[6,7] and extended to include angular forces. Since the EAM potentials apply well to fcc crystals, the MEAM potential was designed to apply to bcc, hcp, diamond-structured materials, and gaseous elements. Also, the free surfaces are better addressed from the MEAM potentials; hence, with regard to the applications related to damage, fracture, and fatigue, the MEAM potential is more attractive.

Atomistic simulations of a wide range of elements and alloys have been performed using the MEAM potentials. Baskes[4] first proposed the MEAM potential to obtain realistic shear behavior for silicon and then Baskes[5] developed MEAM potentials for 26 different elements of the periodic table. The MEAM potential was also applied to numerous cubic materials with various impurities but, for the sake of brevity, they are not included in this document.

Probably the best modern description of the MEAM potential with its associated parameters and

(Published online December 23, 2014)

usage is in Nouranian et al.[8] Also, the MEAM Potential Calibration (MPC) was conducted using large-scale atomistic/molecular massively parallel simulator (LAMMPS),[9] a molecular dynamics code.

CALIBRATING MEAM POTENTIALS

Despite its remarkable successes, one of the most notable difficulties in using MEAM, as well as any of the alternative modern potentials, is that the model calibration of the MEAM potentials historically involved a lot of manual and ad hoc calibrations starting with the original work.[5] Recently, multi-objective optimization formulations in Refs. 10 and 11 have allowed a computational strategy to explore the space of parameters with large datasets (see https://icme.hpc.msstate.edu/mediawiki/index.php/Nanoscale for tutorials to calibrate MEAM with these formulations). However, these complex formulations typically treat all of the parameters at the same time with all of the lower length scale simulation results or experimental data. This paper presents a step-by-step calibration methodology that is straightforward and simple to use, along with its implementation in an interactive software tool.

To fully characterize a MEAM potential, lower length scale information is needed. For this case study, DFT calculations were performed using the Vienna *ab initio* Simulation Package (VASP) to produce FCC, BCC, HCP, elastic constants (C44, C11, C12), vacancy formation energy (VFE), and generalized stacking fault energy (GSFE) data for a pure aluminum system to be used as calibration standards for a MEAM potential. The parameter values in Ref. 12 were used to initialize the MEAM calibration.

The MPC tool's menu items provide the outline of the calibration workflow. The flow essentially is to click the menu items from left to right, and, for each item, click the sub-menus from top to bottom.

Step 1. LAMMPS: select the LAMMPS executable, the working directory, the initial LAMMPS library and parameter files.

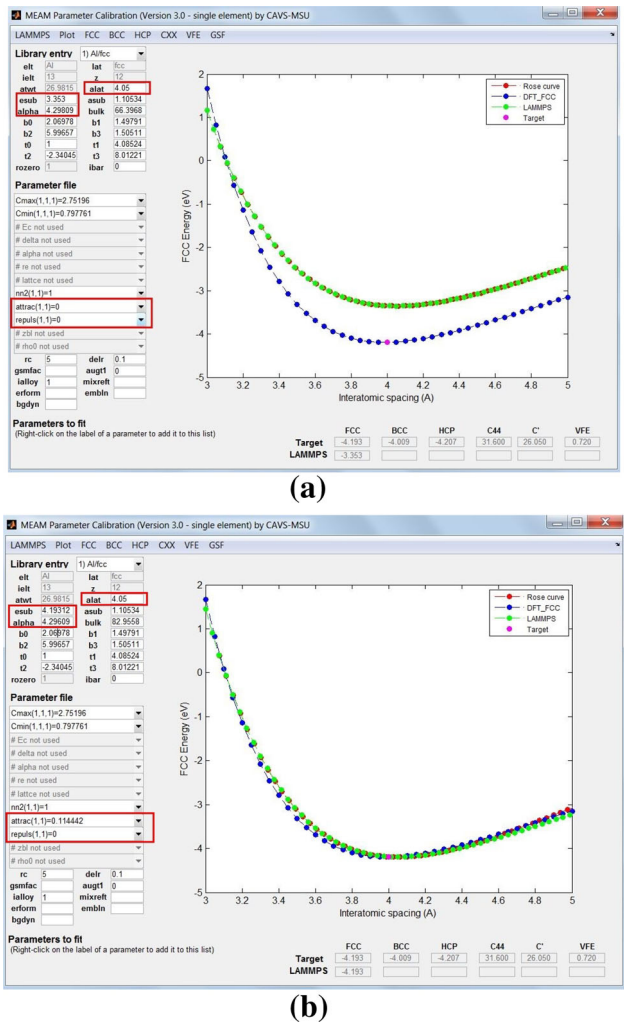

Fig. 1. (a) Initial LAMMPS output for the uncalibrated state, and (b) FCC energy curve output after calibration.

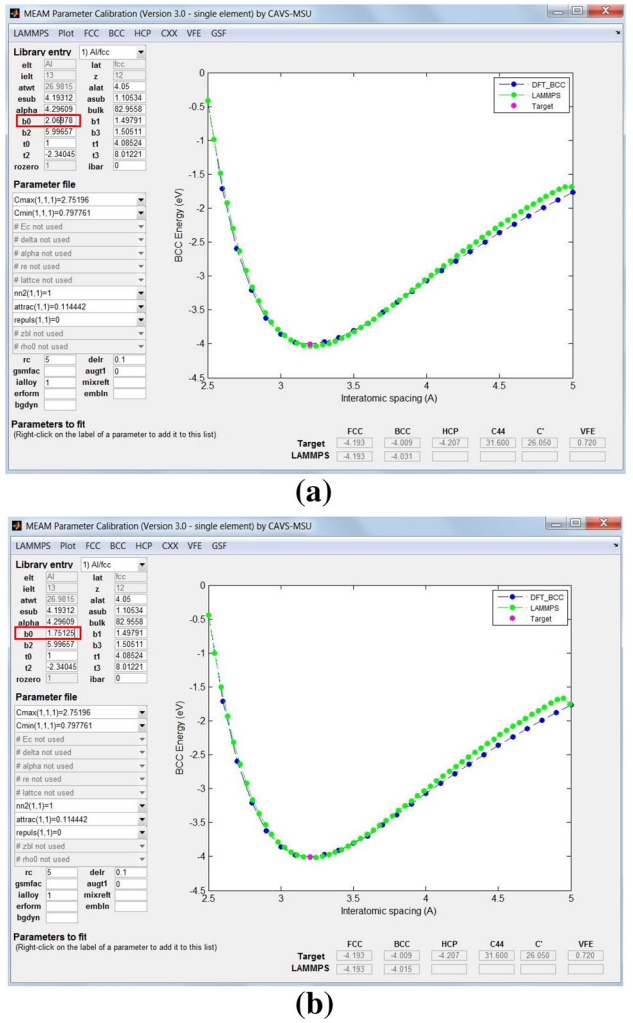

Fig. 2. (a) Initial LAMMPS output for the uncalibrated state to solve for b0 for the BCC crystal, and (b) BCC energy curve output after calibration.

Step 2. calibration to FCC energy versus lattice spacing: load the FCC curve from DFT; calibrate alat, esub, and alpha for LAMMPS to match the minimum FCC energy; calibrate attrac and repuls to fit points away from the minimum.

Using DFT calculation results, we can obtain the energy versus lattice spacing for a FCC crystal lattice. The FCC crystal lattice is chosen first because, for aluminum, it represents the lowest energy and the most stable atomic configuration. If another element such as magnesium or iron were the material of choice, the most stable configurations would be HCP and BCC, respectively. We first start the MEAM calibration by bringing in the Universal Equation of State (UEOS)[13] and then bring in the DFT results as shown in Fig. 1a. By varying the equilibrium lattice constant (alat), energy per unit volume (esub), and bulk modulus-related constant (alpha), we can minimize the error between the DFT target data and MEAM potential at lattice constants near equilibrium. One can either determine the alat, esub, and alpha terms by DFT results or experimental data. The bulk modulus (bulk) is automatically calculated in this implementation from alpha. However, there may be considerable error at lattice constants far from equilibrium. As such, variation of the "attrac" and "repuls" parameters are necessary to reduce the errors. The calibration from fitting alat, esub, alpha, attract, and repuls is shown in Fig. 1b. Figure 1 shows that the final calibrated value for alat is 4.05, esub is 4.19312, alpha is 4.29609, attract is 0.114442, and repuls is 0.0.

Step 3. calibration to minimum BCC energy: load the BCC curve from DFT or experimental BCC energy; calibrate b0 parameter for LAMMPS to match the BCC energy.

From either a lower length scale calculation (e.g., DFT) or experiments, the next step is to determine the energy versus lattice spacing relation for a BCC crystal lattice. Here, one varies the b0 parameter to calibrate to the minimum BCC energy garnered

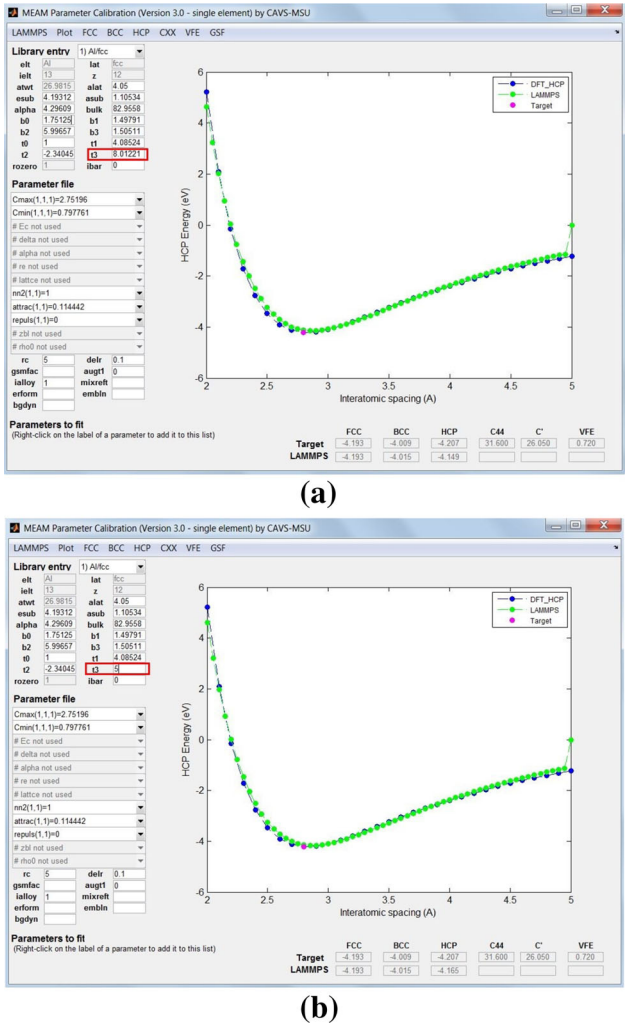

Fig. 3. (a) Initial LAMMPS output for the uncalibrated state to solve for *t*3 for the HCP crystal, and (b) HCP energy curve output after calibration.

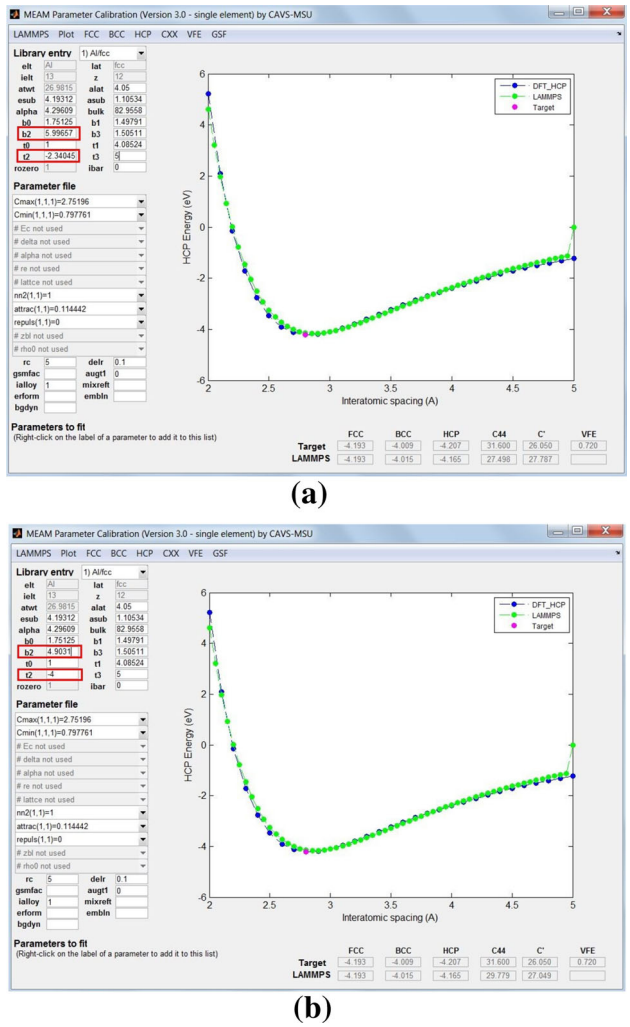

Fig. 4. (a) Initial LAMMPS output for the uncalibrated state to solve for *t*2 and *b*2 for the elastic moduli, and (b) *t*2 and *b*2 for the elastic moduli after calibration.

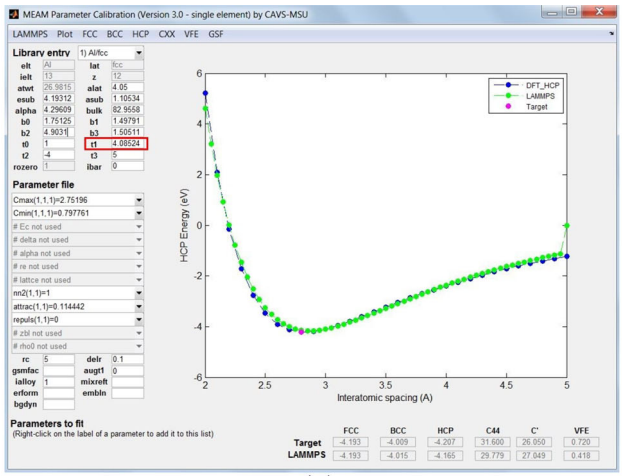

(a)

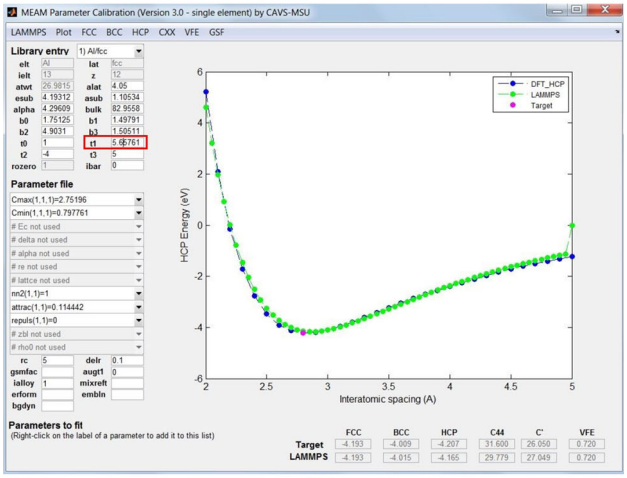

(b)

Fig. 5. (a) Initial LAMMPS output for the uncalibrated state to solve for $t1$ for the vacancy formation energy (VFE), and (b) $t1$ for the VFE after calibration.

from VASP simulations. Figure 2 shows that the initial guess for b0 was 2.06978 but the calibrated MEAM b0 parameter was 1.75125 for aluminum.

Step 4. calibration to minimum HCP energy: load the HCP curve from DFT or experimental HCP energy; calibrate $t3$ parameter for LAMMPS to match the HCP energy.

From either a lower length scale calculation (e.g., DFT) or experiments, the next step is to determine the energy versus lattice spacing relation for an HCP crystal lattice. Here, one varies the $t3$ parameter to calibrate to the minimum HCP energy. Figure 3 shows that the initial guess for $t3$ was 8.01221 but the calibrated MEAM $t3$ parameter was 5.00 for aluminum.

Step 5. calibration to elastic constants C44 and C′: load the elastic moduli C44, C11 and C12 from DFT results or experimental results; calibrate $t2$ and $b2$ for LAMMPS to match C44 and C′ = (C11−C12)/2.

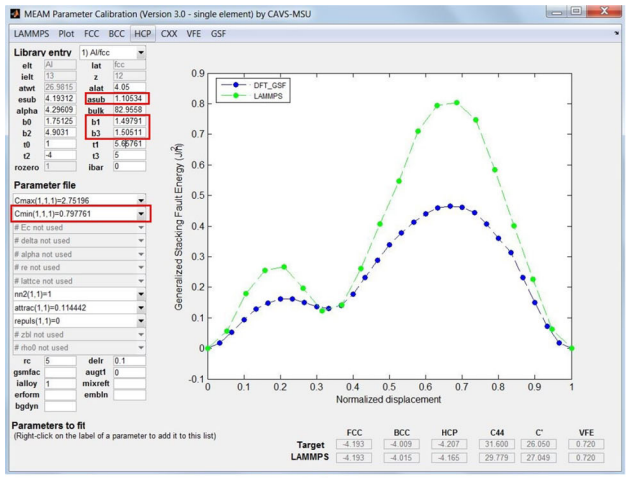

(a)

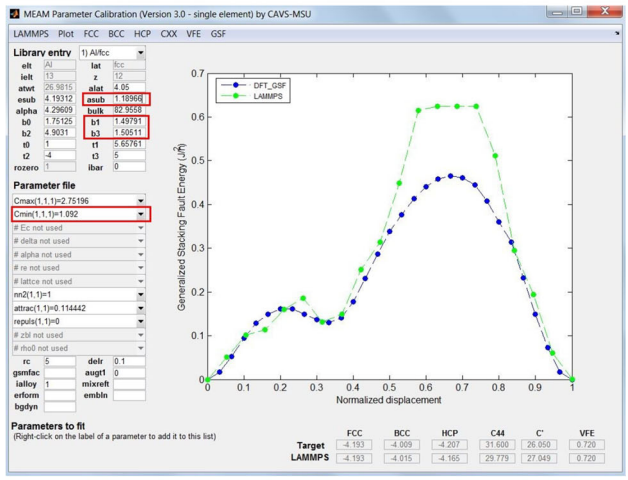

(b)

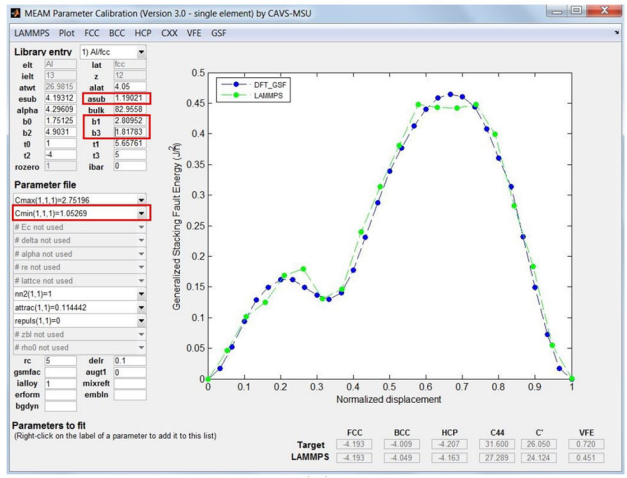

(c)

Fig. 6. (a) Initial LAMMPS output for the uncalibrated state to solve for Cmin, asub, $b1$, and $b3$ for the generalized stacking fault energy (GSFE) curve, (b) Cmin and asub were calibrated to the first maximum and minimum of the GSFE curve, and (c) $b1$ and $b3$ were calibrated to the second maximum of the GSFE curve for aluminum.

Table 1. MEAM model parameter values resulting from calibration to DFT results

Name	Calibrated value	Name	Calibrated value
alat	4.0500	t0	1.0000
esub	4.1931	*t*1	5.6576
asub	1.1902	*t*2	−4.0000
alpha	4.2961	*t*3	5.0000
b0	1.7512	Cmax	2.7520
*b*1	2.8095	Cmin	1.0527
*b*2	4.9031	attrac	0.1144
*b*3	1.8178	repuls	0

From either a lower length scale calculation (e.g., DFT) or experiments, the next step is to determine the elastic constants C44, C11, and C12 (C′ = (C11−C12)/2). Here, one varies the *t*2 and *b*2 parameters to calibrate to the elastic moduli. Figure 4 shows that the initial guesses for *t*2 and *b*2 were −2.3404 and 5.9965, respectively, but the calibrated MEAM *t*2 and *b*2 parameters were −4.00 and 4.9031 for aluminum.

Step 6. calibration to vacancy formation energy: load the VFE target from DFT or experiment; calibrate *t*1 for LAMMPS to match.

From either a lower length scale calculation (e.g., DFT) or experiments, this step is to determine the *t*1 parameter for the VFE.). Here, one varies the *t*1 parameter to calibrate to the VFE. Figure 5 shows that the initial guesses for *t*1 was 4.0852, but the calibrated MEAM *t*1 parameter was 5.65761 for aluminum.

Step 7. calibration to generalized stacking fault energy (GSFE) curve: load the GSFE curve from DFT; calibrate Cmin and asub for LAMMPS to match the first local maximum; calibrate *b*1 and *b*3 for LAMMPS to match the second local maximum.

One can obtain a GSFE curve from a lower length scale calculation. The parameters Cmin and asub can be varied and LAMMPS iteratively run to determine the GSFE curve until a good calibration between the LAMMPS results and the lower length scale data is found. As Fig. 6b shows, Cmin and asub are related to the first maximum and minimum of the GSFE curve indicating that these two parameters are related to the unstable dislocations (first maximum) and stable dislocations (minimum). Later, one can vary *b*1 and *b*3 to capture the second maximum of the GSFE curve, which is sometimes related to deformation twinning. Figure 6c shows the comparison once *b*1 and *b*3 were modified. The initial values for Cmin, asub, *b*1, and *b*3 were 0.7977, 1.1053, 1.4979, and 1.5051, while the calibrated values were 1.05269, 1.19021, 2.80952, and 1.81783, respectively.

After the calibration of one parameter or a subset of the parameters, a right-click on an empty space in the interface will reveal a context menu from which a submenu entry may be selected to regenerate, in a single step, all LAMMPS plots based on the current set of parameters. For the present case study, a few iterations of steps 2–7 may still be necessary to better fit the BCC, HCP, C44, and C′ targets.

SUMMARY

A calibration methodology for determining the MEAM potential garnered from information from *ab initio* calculations (and experimental where available) that was focused on dislocation effects was presented in this article. An interactive graphical MATLAB program called the MPC tool was created to help the user quantify the different parameters for a single element MEAM potential. Although the example used here was aluminum, the MPC tool can easily be used for other elements of the periodic table. Also, an extension to multiple elements is forthcoming. The tool can be retrieved from the website: https://icme.hpc.msstate.edu/mediawiki/index.php/Nanoscale. Also, since the focus of the multiscale bridging effort was related to dislocation dynamics at the next higher length scale, we focused on the GSFE curve, but other metrics in the ICME philosophy, such as the heat of formation, could be used instead depending on the downscaling requirements. Table 1 presents a summary of the calibrated MEAM parameter values using the calibration routine.

ACKNOWLEDGEMENTS

The authors would like to acknowledge the Center for Advanced Vehicular Systems (CAVS) at Mississippi State University for support of this work.

REFERENCES

1. J. Allison, M. Li, C. Wolverton, and X.M. Su, *JOM* 58 (11), 29 (2006).
2. M.F. Horstemeyer, *Integrated Computational Materials Engineering (ICME) for Metals: Reinvigorating Engineering Design with Science* (Hoboken, NJ: Wiley Press, 2012).
3. S. Groh, E.B. Marin, M.F. Horstemeyer, and H.M. Zbib, *Int. J. Plast.* 25, 1456 (2009).
4. M.I. Baskes, *Phys. Rev. B* 59, 2666 (1987).
5. M.I. Baskes, *Phys. Rev. B* 46, 2727 (1992).
6. M.S. Daw and M.I. Baskes, *Phys. Rev. B* 29, 6443 (1984).
7. M.S. Daw, S.M. Foiles, and M.I. Baskes, *Mater. Sci. Rep.* 9, 251 (1993).
8. S. Nouranian, M.A. Tschopp, S.R. Gwaltney, M.I. Baskes, and M.F. Horstemeyer, *Phys. Chem. Chem. Phys.* 16, 6233 (2014).
9. S.J. Plimpton, *J. Comput. Phys.* 117, 1 (1995).
10. S.G. Kim, M.F. Horstemeyer, M.I. Baskes, M. Rais-Rohani, S. Kim, B. Jelinek, J. Houze, A. Moitra, and L. Liyanage, *J. Eng. Mater. Technol.* 131, 041210 (2009).
11. M.A. Tschopp, K.N. Solanki, M.I. Baskes, F. Gao, X. Sun, and M.F. Horstemeyer, *J. Nucl. Mater.* 425, 22 (2012).
12. B. Jelinek, S. Groh, M.F. Horstemeyer, J. Houze, S.G. Kim, G.J. Wagner, A. Moitra, and M.I. Baskes, *Phys. Rev. B* 85, 245102 (2012).
13. J.H. Rose, J.R. Smith, F. Guinea, and J. Farrante, *Phys. Rev. B* 29, 2963 (1984).